Universitat de les Illes Balears

Robustness of Plant-Pollinator Mutualistic Networks to Phenological Mismatches

Clàudia Payrató Borràs

Master Thesis

Academic Year 2015-2016

Master's Degree in Physics of Complex Systems

at the

UNIVERSITAT DE LES ILLES BALEARS

SUPERVISOR: **José Javier Ramasco**

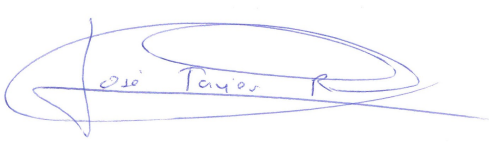

AUTHOR'S SIGNATURE:

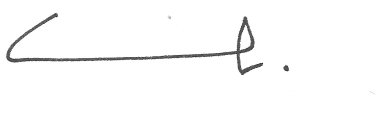

Date: 9th September 2016

Acknowledgments

In the first place, I would like to especially thank my thesis supervisor, José Javier Ramasco, for his advise, guidance and continuous help.
Also thank you to the rest of the IFISC crew for their warm welcome.
And last but not least, many thanks to the Zulo's team.

Abstract

Mutualistic interactions conform the skeleton of many systems widespread in nature, with abundant examples ranging from the economical context to the biological world. The paradigmatic case of study -and ours- is ecological networks. The singular composition of their interactions is known to exhibit unique resilient features, playing a critical role to the preservation of earth's biodiversity and ecosystem's robustness. However, the extent to which the so-called mutualistic networks might be affected by global change has still not been well-established. Accordingly, in this Master Thesis we attempt to measure the robustness of a plant-pollinator community to shifts in their life cycles (phenologies). By borrowing tools from population dynamics and statistical mechanics, we characterise a phase transition triggered by phenological noise in a non-spatially extended model. Our results suggest the existence of a second order non-equilibrium phase transition. Moreover, simulations on an empirically-based network successfully reproduce some previously known ecological traits. All in all, many critical features attributed to second-order transitions such as scaling or universality remained to be asserted, thus demanding for further investigations.

Contents

Chapter 1

Introduction

1.1 Mutualistic networks in a nutshell

Our understanding of the way in which mutualistic interactions are capable to shape the structure and function of ecosystems has undergone a unique, and almost revolutionary evolution during the last two decades. Such progress responds to a great extent to a transformation of the paradigm in which mutualism is conceived: instead of centering the attention on the details of how a single one-to-one interplay may occur, the focus has been placed on capturing the essentials of the whole network of interactions. This change of perspective, that encounters analogues in many other fields from sociology to systems biology, permitted to unveil a profound and vital connection between the organisation of mutualistic links and elementary ecological features, such as biodiversity maintenance or ecosystem's robustness.

In this section we present the framework in which this novel paradigm of mutualistic networks is embedded, as well as the main results of the research carried out, principally by J. Bascompte and colleagues. We start explaining the construction of a mutualistic network and characterising one of its essential features: nestedness. Secondly, we turn our attention to the key ecological properties related to nestedness and, of particular importance for our work, its repercussions on network's robustness.

Figure 1.1: Representation in a bipartite network of a small plant-pollinator mutualistic community. Width of links represents its variable weight.

Mutualistic communities are usually depicted using *bipartite networks*. This type of network is formed by two different set of nodes representing the two classes of agents involved in the mutualistic relationship (which can range from plants and their pollinators to manufacturers and contractors). For models that are not spatially-extended like ours, each node portraits a population's specie, while links depict the interactions with their counterparts, as shown in Fig. 1.1. In addition, edges might be weighted when the benefit that each specie obtains from the interaction is known or is being modelled.

This translation of an ecological system into the language of networks permitted to address the question of how links are organised, revealing a highly non-random pattern of interaction. Indeed, Bascompte et al. [1] demonstrated that empirical networks are strongly *nested*. Nestedness is a global measure of structure, that estimates what distance separates a specific distribution under study (for instance Fig. 1.2b), from an ideal composition in which species with large degrees (generalists) do not exclusively associate among them but also contain a subset of links to low-degree nodes (specialists), resulting in a macroscopic configuration of the sort shown in Fig. 1.2a.

As already outlined in [1], from these remarkably non-trivial configurations we might expect special dynamical properties. For instance, the existence of a cohesive core of generalists (see Fig. 1.2a) should

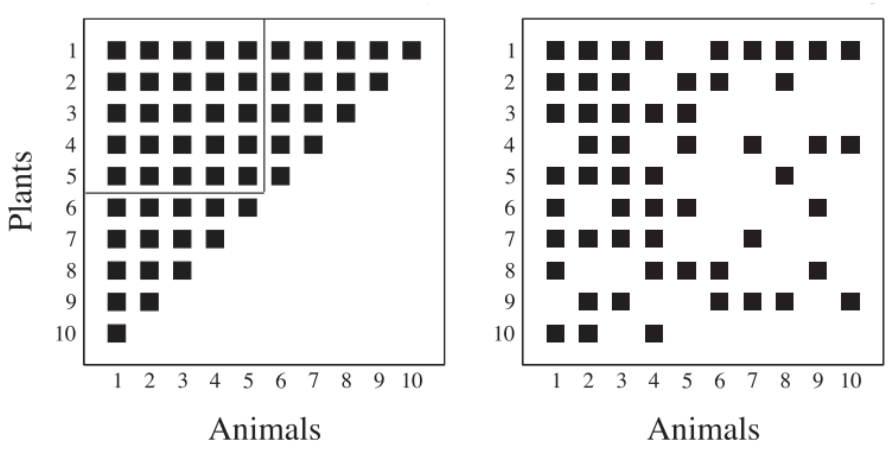

(a) Perfectly nested community. (b) Poorly nested community.

Figure 1.2: Two communities of plants and pollinators, one of them perfectly nested (a), and the other one with a randomised distribution of interactions (b). Plants and animals are labelled with their rank, being 1 the specie with more interactions and 10 the one with less. Black squares are placed when there is an interaction. Finally, the box in a frames the core of the network, formed by species interacting all-to-all. Pictures extracted from [1].

provide enhanced robustness, as well as warrant a greater change of survival to specialist species attached to it.

In fact, this finding triggered a sequence of fundamental discoveries, aimed at constructing a bridge between the observed structural pattern and other essential ecological measures. For instance, it was shown that biodiversity maintenance is enhanced both by an asymmetric nature of the interactions [2] and a palliation of interespecific competition due to a nested organization [3]. Besides, coextinction cascades were found to occur in a structured manner, depending strongly in their phylogenetic history together with the network architecture [4].

Finally, a crucial question that arises from this discussion is what the stability of a mutualistic network is, and how much it is conditioned by the nature of the interactions and its assemblage. This might be of special importance for our work, in which the stability of a plant-pollinator network is threatened by the presence of phenological noise. In this sense, Thébault and Fontaine [5] proved that a nested architecture favours the resilience of networks subject to mutualism, but instead diminishes the dynamical stability of other models such as trophic communities.

Among other relevant results that we could no sum up here, these ideas might give a taste of the type of research that have been developed on mutualistic networks over recent years, and how they have shed light on many unknown connections between ecological macroscopic properties such as biodiversity, and the unique composition formed by mutualistic interactions.

1.2 The fate of mutualism

Given the vital role that mutualism plays in maintaining biodiversity as well as in warranting some communities' stability, it is inevitable to ask whether such type of networks are resilient to external perturbations, and in general, how they may respond to them. Nowadays, climate change is a worldwide threat from whose effects plant-pollinator networks will be most probably unable to scape. Actually, some of the first consequences of global warming on the functioning of biological communities have already been reported, as we now expose.

The repercussions of climate change can not always be easily unravelled, and indeed different factors might act synergetically leading to an enhanced stress than the one caused from their individual actions. However, as exposed by Hegland et al. [6], in plant-pollinators systems the most significant alterations appear on species' abundance and distribution, and secondly on the cycles of flowering and birth (whose study is usually known as *phenology*). Because we are concerned with a non-spatial model, we will focus primarily on phenological perturbations.

Numerous empirical studies have asserted the fact that species' phenology can be greatly affected by an environmental warming [6]. In particular, both the onset of flowering and the date of first emergence of insects seem to be positively correlated with temperature, exhibiting an almost linear response for plants and bees (see Fig. 1.3), as well as a singular connection with the previous-month temperature in the case of butterflies. Also the period of activity appears to be altered, yet no clear consensus has been reached since observations are controversial among them.

An immediate consequence of these phenological perturbations -usually called *phenological shifts*- is the possibility that periods of activity desynchronise between interacting agents, resulting in what is known as *phenological mismatches*. From this, two fundamental questions naturally arise: first, what is the gravity of the damage that such loss of overlap may cause on the community? Second, what is the future of phenological mismatches? Are they destined to keep increasing due to a persistence of the linear tendency to shift, or will they be damped at some moment by a coevolutionary feedback from the community (see Fig. 1.3)? On these two issues relies, to a great extent, the fate of mutualism.

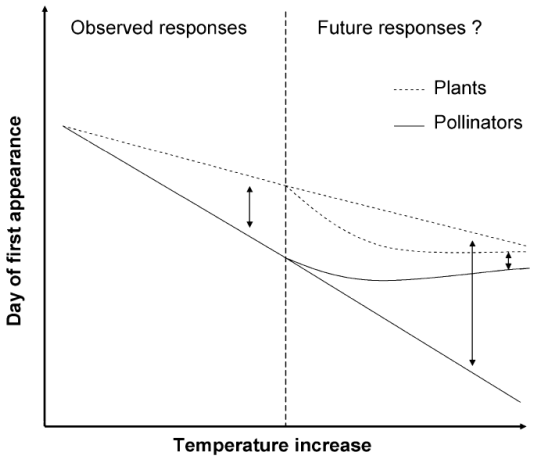

Figure 1.3: Response of plants and pollinators to temperature increase. The observed response is inferred from experimental findings, and phenological mismatches (marked by the doble arrow) may occur due to a different slope in the linear response to temperature increase. The right part of the plot depicts various plausible scenarios. If the observed tendency is maintained, phenological mismatches will imperatively increase (large doble arrow). Instead, if coevolutionary processes counteract phenological shifts, then the resulting mismatch might be diminished. Plot borrowed from [6].

Consequently, over the last ten years researchers have struggled to provide a definitive answer, both experimentally and theoretically. Our aim in this thesis is to address the first subject, on which much light has already been shed. To start with, Memmott et al.[7] showed by simulating phenological shifts on an empirical network that, if the current observed shifting tendency is maintained, then the amount of overlap do certainly decrease, eventually risking the survival of its species. Indeed, Burkle et. al. [8], analysed a large historical data set and concluded that phenological shifts may account, together with species extirpation and habitat loss, for a severe degradation of the network structure leading to less resilient configurations. Apart from these two examples, not few others exist, though we are not able to review them all. For our purpose it will be enough to state that in general, both empirical and modelling approaches seem to converge to the idea that perturbations in phenology significantly affect the functioning of the mutualistic newtork [6].

Chapter 2

Methods

In this chapter we present the methods implemented to model, simulate and measure the effects of phenological mismatches on a mutualistic network. First, we introduce the model used to reproduce population growth in presence of mutualistic interactions and the algorithm for its integration. Next, we illustrate how phenological mismatches can be included into the dynamics of a plant-pollinator system. Then follows the description of the procedure applied to characterise the observed phase transition, and finally we pay some attention to the ecological data used for our calculations, as well as to the parameters' choice.

2.1 Deterministic model with mutualistic interaction

We start by constructing a mutualistic community embedded in a bipartite network like the one we have described before. The theoretical network used in many of our calculations -from now on, unless when stated otherwise- is depicted in Fig. 2.1.

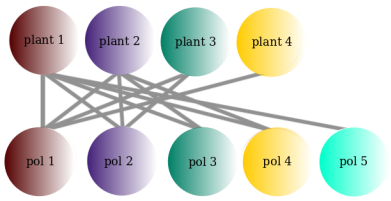

Figure 2.1: Representation of a theoretical network of plant-pollinators. Interactions and parameters as proposed by García-Algarra et al.[9].

The variable in which we are interested is the number of individuals on each node. Therefore, we need of a set of equations that calculates a species' population as a function of the state of the rest of the network, that is, a dynamic equation of population growth. Following the discussion by [9], here we use the present dynamical equations for the growth of plants and pollinators:

$$\frac{1}{N_i^a}\frac{dN_i^a}{dt} = r_i + \sum_{j=1}^{n_p} b_{ij} N_j^p - \left(\alpha_i + c_i \sum_{j=1}^{n_p} b_{ij} N_j^p\right) N_i^a, \tag{2.1}$$

$$\frac{1}{N_j^p}\frac{dN_j^p}{dt} = r_j + \sum_{i=1}^{n_a} b_{ji} N_i^a - \left(\alpha_j + c_j \sum_{i=1}^{n_a} b_{ji} N_i^a\right) N_j^p \tag{2.2}$$

where the superindex p refers to plants, while, to avoid confusion, a stands for animals (pollinators). The intrinsic growth is represented by r, and α acts as a friction term -which, in biological terms, is a consequence of intraespecific competition- that prevents the system from unbounded growth. Finally, mutualism is enclosed in the factors b_{kl}, which represent the benefit obtained by each specie thanks to its interactions with their counterparts.

As can be seen, both the positive and the negative terms contributing to population growth show a dependence on the mutualistic benefit. As discussed in [9], the underlying motivation of this model is similar to the one for the logistic equation: mutualistic components add positively to population growth but are also object of competition, thus needing to be present in the friction part as well. With this idea in mind, García-Algarra et al. showed that such equations can lead to identical dynamical scenarios to the ones produced by the Type II model, whereas allowing a less intricate analytical analysis.

In particular, the stability analysis revealed that there are three possible final regimes for the system: total extinction -all plant and pollinators species die-, partial extinction -a part of the species die, but the rest survive- or full system capacity -all species achieve their carrying capacity limit. When mutualism is facultative for all species ($r_i > 0$, $\forall i$) the only stable fixed point is full system capacity, and total extinction and partial extinctions are unstable points. If mutualism turns obligatory for one of the species ($r_j < 0$ and $r_i > 0$ $\forall i \neq j$) then total extinction becomes a saddle point. However, the most interesting situation to us is when mutualism is obligatory to all species ($r_i < 0$, $\forall i$). In that case, both total extinction and full system capacity are stable fixed points and the phase space is separating its two basins of attraction by a survival watershed, which includes partial extinction as a saddle-node. This means that depending on the initial population values the system will be driven to survival (see Fig. 2.2) or to extinction (see Fig. 2.3).

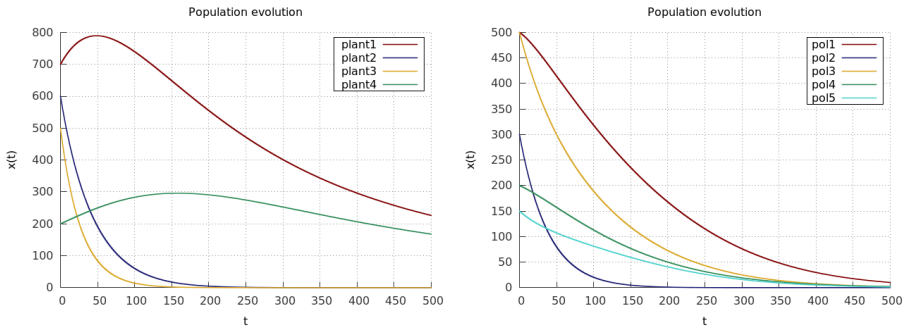

(a) (b)

Figure 2.2: Temporal evolution of the system when working in the parameter region of complete extinction. In (a), plant populations. In (b), pollinator populations. Integration has been done performing with a RGK4 algorithm over the theoretical network in Fig. 2.1 and using the parameters for full extinction provided in [9], that can be found in Appendix A.

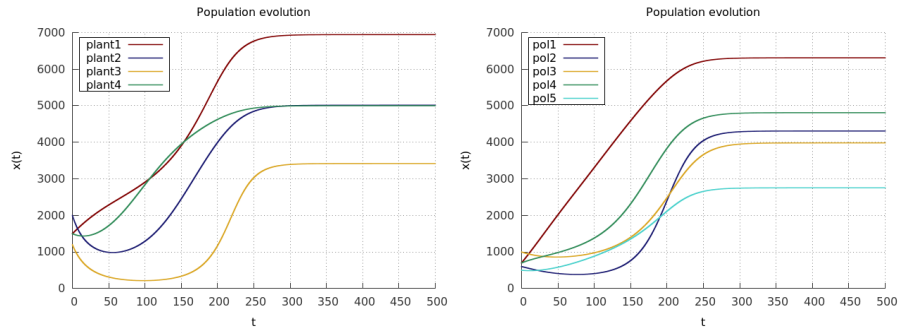

(a) (b)

Figure 2.3: Temporal evolution of the system in the parameter region of full capacity. In (a), plant populations. In (b), pollinator populations. Integration has been performed as in Fig. 2.2, with the parameters that lead to full capacity (see Appendix A).

As outlined by García-Algarra et al., it is significant to recall that for multispecies communities (more than two), partial extinctions consist in projecting the original system to a new point in the flow diagram that, relevantly, may belong to the extinction basin or to the survival one. This means that

partial extinctions may lead the system to an actually surviving state -and possibily more resilient, if its nestedness has increased- or contrarily to a cascade of extinctions, if the reduction of dimensionality repeatedly projects the system on the basin of attraction of the full extinction fixed point. This result is very important to us, since the phase transition will be very much conditioned by the way in which the system collapses after partial extinctions.

In conclusion, we will work with a model of population dynamics inspired on logistic growth in which mutualism regulates both the growth rate and the friction component. We set mutualism being obligatory, so that our parameter space corresponds to a phase space with remarkable richness, including scenarios of total extinction, partial extinction and full survival. This will allow us to simulate transitions between these regimes, relying on the number of individuals of each species as the order parameter.

2.2 New stochastic model

In order to obtain a hopefully more accurate description of our mutualistic system, we propose a new stochastic model which reproduces in the mean-field limit the deterministic behaviour of the model by García-Algarra et al. We propose the existence of two elementary microscopic processes for each species: death or reproduction. Summing over all species, there are $2(N_p + N_a)$ possibilities in total. Let us illustrate it for a plant labelled k. The events that could happen concerning the population of plant k are:

$$N_k^p \to N_k^p + 1 \quad \text{reproduction}, \tag{2.3}$$

$$N_k^p \to N_k^p - 1 \quad \text{death} \tag{2.4}$$

and we propose a model where each of them occurs with the rate:

$$\Omega((N_1^p, ..., N_k^p, ..., N_1^a, ...) \to (N_1^p, ..., N_k^p + 1, ..., N_1^a, ..)) = N_k^p \left(r_k + \sum_{i=1}^{n_a} b_{ki} N_i^a \right), \tag{2.5}$$

$$\Omega((N_1^p, ..., N_k^p, ..., N_1^a, ...) \to (N_1^p, ..., N_k^p - 1, ..., N_1^a, ..)) = (N_k^p)^2 \left(\alpha_k + c_k \sum_{i=1}^{n_a} b_{ki} N_i^a \right) \tag{2.6}$$

To integrate these dynamical equations we implement the Gillespie algorithm [10]. This method provides an exact integration, involving the generation of two random numbers as we now explain (see also [11]):

First, we compute the time interval for the next event to occur as $log(u)/W(N_p, N_a)$, where N_p and N_a are the total number of plants and pollinators. Here u is a $U(0, 1)$ random number while $W(N_p, N_a)$ is the total rate, that is basically the sum of the right hand-side of Eq. 2.1 multiplied by N_i^a and sumed over all animal species, added to the sum of the right hand-side of Eq. 2.2 multiplied by N_i^p and over all plant species. As can be seen, the larger the rate the smaller the average of the interevent time distribution and hence the quicker the system will be evolving in time.

Next, we calculate what of the potential events will be taking place so that the probability that, let's say, plant k reproduces, is its rate Ω divided by the total rate W. Handling the probabilities for all the possible processes and drawing a second random number, we can chose which event will occur. Intuitively we observe again that the greater the rate for one process, the more probable that it will happen.

With this algorithm we obtain an exact integration based on the microscopic dynamics of the system (see Fig. 2.4 and compare with Fig. 2.2). It offers us significant features compared to a deterministic model, such as the existence of absorbing states and the exact representation of the discrete character of populations. Indeed, these turn out to be relevant processes in the context of small populations, which is in fact the scenario that we will found when approaching extinction.

To finish, it is interesting to remark that the step from the deterministic model to a set of microscopic processes is not unique nor unidirectional, and we could have proposed as well other microscopic models reproducing the same mean field features. In the end, the election of one model over another should be related to its accuracy in biological terms, that is, to the realism of the chosen representation.

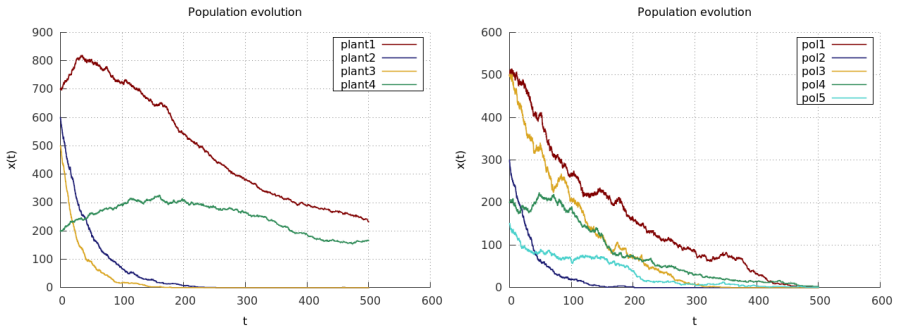

(a) (b)

Figure 2.4: Temporal evolution of the system when working in the parameter region of complete extinction, using the same parameters as in Fig. 2.2. In (a), plant populations. In (b), pollinator populations. Integration has been performed using Gillespie algorithm.

2.3 Simulation of phenological mismatches

As we have discussed before, phenological mismatches occur when the period of flowering of a plant and the period of activity of its pollinator fail to overlap, partly or entirely. In consequence, if they do not coincide in time, mutualistic partners are unable to interact and their dynamics should be affected somehow.

One possibility to model the effects of such mismatch could be to simulate the desynchronization of the temporal dynamics explicitly, that is, to switch off the link of interaction while they do not coincide, and switch them on again (preserving their normal weight) at the moment there is overlap. However, such procedure assumes that the equation is microscopically exact, which is something, as we have suggested previously, not completely assured.

Therefore, we adopt the approach of considering the coefficients under a mean-field perspective, not only regarding the nature of the interaction but also in a temporal sense. This means that the effect of diminishing the overlap during one spring is represented by a reduction on the mutualistic coefficient for that interaction (b_{ij}, see Eqs. 2.1-2.2) in the whole year. In this sense, we consider that failing to interact does not have an immediate consequence, but a time-distributed response. In the network language this would correspond, instead to connecting and disconnecting links, to a continuous variation of the link's weights.

Knowing this, the detailed calculation of the coefficients for mutualistic benefit is as follows:

Initially, the matrix b_{ij} is set so that all species work on the regime of full capacity. Each specie has a period of activity assigned, and the initial time of flowering (for the plants) and birth (for the pollinators) is such that the overlap is maximum (later on we explain how we generate those times). This initial time corresponds to $t_{i,0}$ on Fig. 2.5.

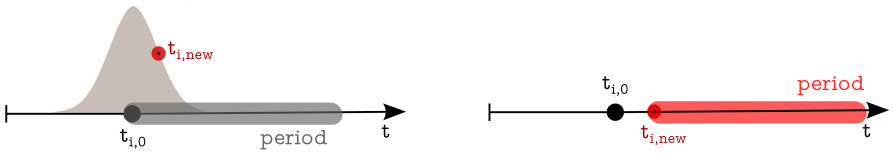

Figure 2.5: Representation of the process of construction of the new phenology. On the left, initial flowering/birth time, $t_{i,0}$, and the period of activity. The red point indicates a random number drawn from a Gaussian distribution around the original initial time. On the right, shifted phenology due to relocation of the period of activity, starting then on $t_{i,new}$.

Then, we introduce the phenological shift by generating a new initial time (in days) of flowering or birth ($t_{i,new}$ on Fig. 2.5). This new time is obtained from a Gaussian distribution of standard deviation σ (measured in days) and centred on $t_{i,0}$. Next, we move the period of activity in time while keeping, for simplicity, its duration unchanged. This leads to a new phenological overlap between

the two species, that may correspond to any of the three situations depicted in Fig. 2.6: full overlap, partial overlap or no overlap.

According to the final quantity of overlap, we set the value of the mutualistic benefit as the portion of actual period of coincidence, divided by the maximum possible period of coincidence (which is the length of the shortest of the two periods). This offers a continuous range of variation for b_{ij}, from its maximum value -when there is full overlap- to zero -when there is absolutely no coincidence-.

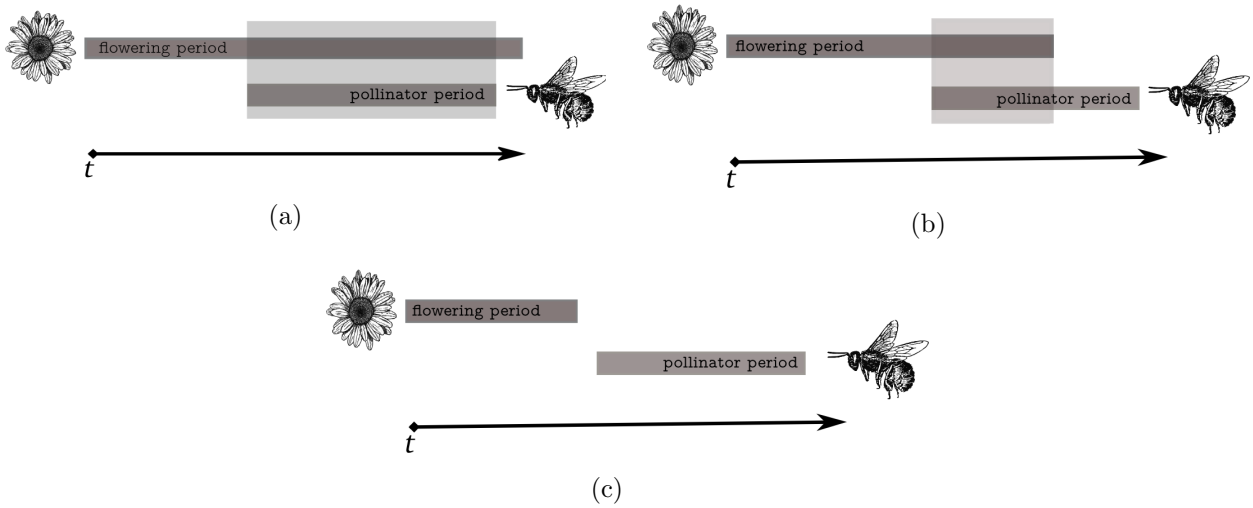

Figure 2.6: Qualitative cases of overlap. In (a), full coincidence when the shortest period falls inside the period of its partner specie. In (b), partial overlap when the shortest period falls partly out of the largest period. In (c), no overlap at all. Pollinator's periods of activity do not necessarily need to be shorter than plant's ones, although being the case in this example.

Initial time distribution

A key element of this procedure is the generation of a set of initial times of birth and flowering which fulfil that the overlap between all species is maximum. Because of the complexity of the networks of interaction, this optimizing problem has non-unique solutions.

The trivial solution is a distribution in which all times are centred around the same value, in other words, when all the middle times of activity coincide (see Fig. 2.7). We can construct such distribution by assigning an initial time zero to the specie with the longest period. Then, the rest of initial times are immediately set using the same center time. This procedure ensures that all species overlap among them.

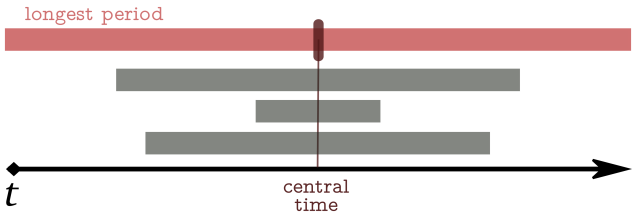

Figure 2.7: In pink, longest period of activity. Its middle time is marked in dark red. This is also the center time around which the rest of periods are located.

Nonetheless, in the construction of this solution we pay the price of presuming some rigid characteristics that, as we will discuss in the next chapter, might not be empirically faithful. Thus, we now explain how to generate other solutions using a numerical method that does not require any limiting assumption.

The method used is the package *Differential Evolution* from the *SciPy* library by Python [12]. The algorithm minimises a given function (which in our case is $1-p$, where p is the normalised sum over all

overlaps) in a given interval (which we set as the spring season), by iteratively improving a candidate solution. Without entering in much detail, this is achieved by comparing a first candidate -drawn from a random choice over the whole population- with a trial vector -formed by random mutations over the candidate-, and then selecting the best out of the two as the new candidate. This process is iterated until an optimal solution is found.

One of the drawbacks of this method is that convergence is slow and requires a larger number of evaluations of the optimizable function than other numerical algorithms. Anyhow, since the distributions of times need to be generated only once, this is not a computational inconvenience for us. On the contrary, the method offers great advantages such as not relying on a gradient for the optimisation as well as being stochastic in nature, which permits us to explore the solution space and thus to generate different pseudo-optimal solutions.

Long runs

Up to now we have exposed a manner of simulating an isolated phenological shift. In reality, we are interested in measuring the response of the network to continuous perturbations of its species' phenology, since momentary mismatches are most probably unable to bring the system to a collapse.

To test the resilience of the system to repeated phenological mismatches, we first integrate the dynamics of the network without noise, until each specie has reached its carrying capacity limit. This *thermalizing* period corresponds to the first stage observed in Fig. 2.9 (up to $t = 500$ years), and we can check that it is independent of the value of σ. Next, we introduce the phenological shifts as discussed above, and recalculate accordingly the values of b_{ij}. The perturbed coefficients are used to integrate the dynamics during the time corresponding to a whole year, and then new phenological shifts are generated using the same standard deviation. For simplicity, we assign an identical σ value to all species in the network.

In this second stage, the system is driven to a new steady state, as can be observed in Fig. 2.9. Furthermore, a comparison among those single runs suggests that increasing the value of σ leads the system from species survival to their extinction. These preliminary results are the first indication of the presence of a phase transition, and consequently of the existence of a critical value of σ beyond which the network collapses.

2.4 Characterisation of the phase transition

In order to assert the existence of a phase transition, we need an accurate measure of the steady state in presence of noise.

Due to the stochastic nature of the integration method as well as of the phenological shifts, we first perform an average over various runs. Not only the processes but also inter-event times are stochastic. Thus, the average is carried out by coarse-graining the trajectories on a grid of width $\delta t = 1.0$ years, as shown in Fig. 2.8, and then averaging over the states of the system at the intersections with the grid, which are the grey points on $t_1, t_2, ...$ of Fig. 2.8.

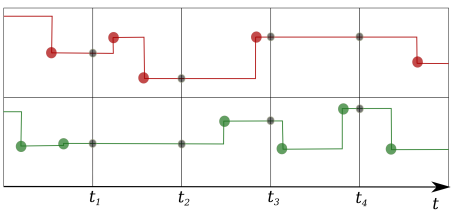

Figure 2.8: In pink and green, two single stochastic trajectories. Grey points represent the points to be averaged, that are defined by the last event before the intersection with the grid.

To obtain a proper measure of the steady state we need to pay an special attention to the problems that arise around the critical region. In particular, there are two main issues to take into account in a second-order non-equilibrium phase transition (as we will prove that we have): increase of fluctuations and finite size effects.

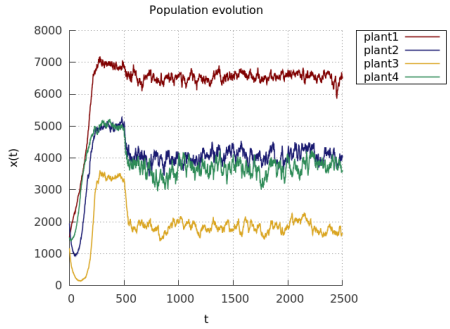

(a) $\sigma = 7.00$. Plants.

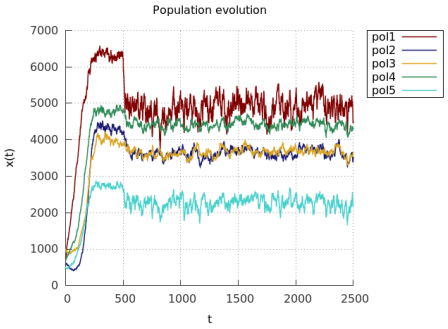

(b) $\sigma = 7.00$. Pollinators.

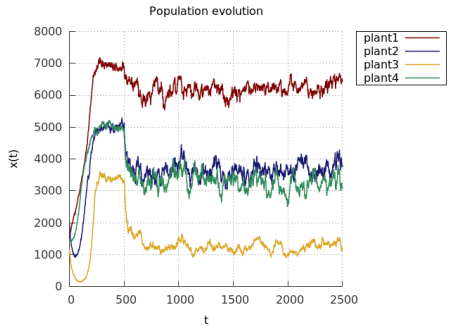

(c) $\sigma = 9.00$. Plants.

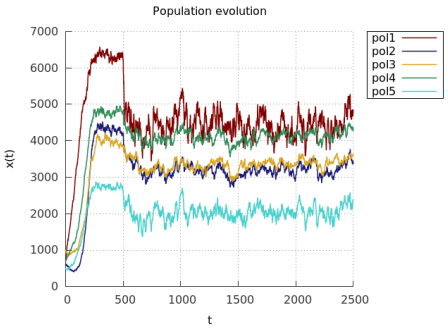

(d) $\sigma = 9.00$. Pollinators.

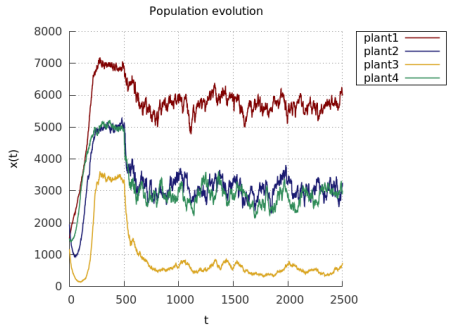

(e) $\sigma = 11.00$. Plants.

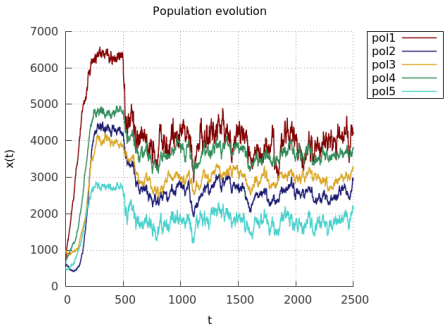

(f) $\sigma = 11.00$. Pollinators.

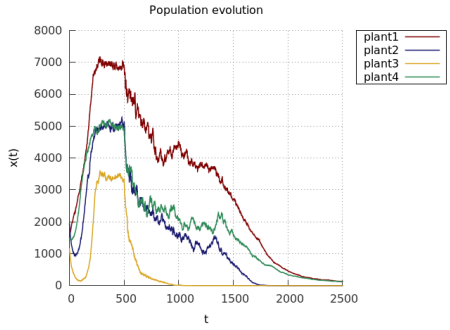

(g) $\sigma = 13.00$. Plants.

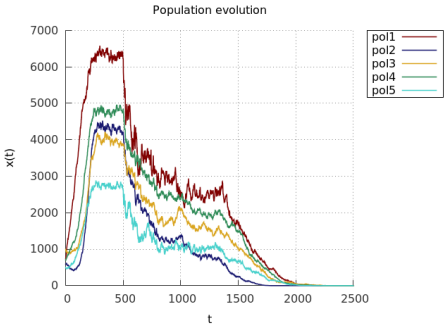

(h) $\sigma = 13.00$. Pollinators.

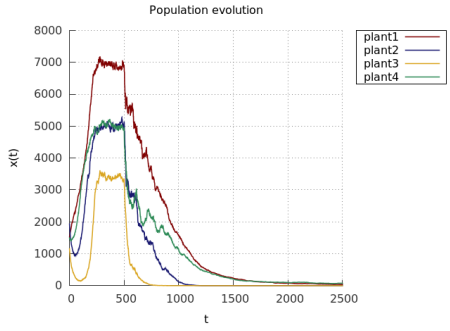

(i) $\sigma = 15.00$. Plants.

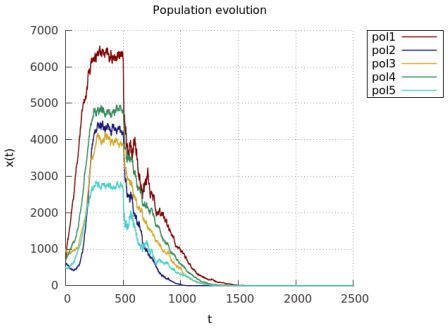

(j) $\sigma = 15.00$. Pollinators.

Figure 2.9: Single runs of the time evolution of plants and pollinators for different amplitudes of phenological noise σ.

As outlined by [13], the increase of fluctuations is due to the relation between the response function and the statistical error of the order parameter. In a second-order non-equilibrium phase transition, response functions diverge at the critical point and so does the variance of the order parameter, which in our case is the total population. In fact, because of finite-size effects, such fluctuations can not actually diverge, yet they become large enough to lead the system to absorbing states. In order to solve these problems, we perform the average only over the *active* runs (N_{act}), discarding from the normalisation the *absorbed* runs that do not respond to real extinctions but are a consequence of finite-size effects. Moreover, we increase the number of iterations close to the critical zone in order to reduce statistical error. All in all, the sampling is constricted by the size of the network, because larger networks demand a much longer computational time, which limit in practice the number of doable repetitions.

As shown in Fig. 2.10, the total population rapidly evolves to a new steady state at which remains almost constant, while the number of active runs exponentially decays to zero. It can also be noticed that when N_{act} becomes very small, the fluctuations of the order parameter increase since the sampling size of runs is significantly lower.

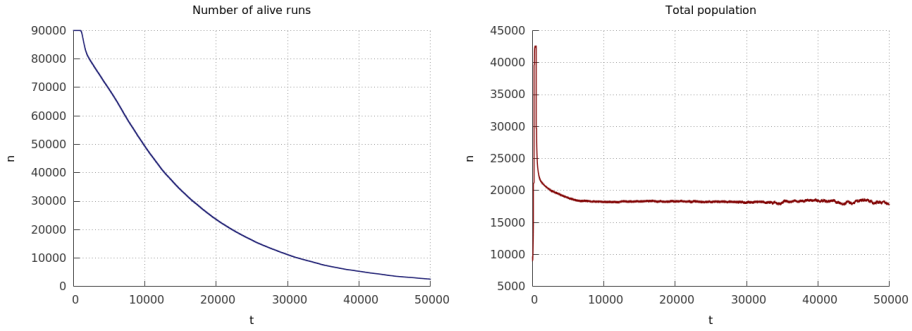

(a) Number of active runs. (b) Total population.

Figure 2.10: Total population and number of active runs as a function of time for a value of the phenological noise $\sigma = 12.50$.

In consequence, the optimal region to perform the measures is that in which we have already reached the steady state but the number of alive runs is still large. Observing Fig. 2.10, we can conclude that integrating until $t_{max} = 10^4$ we accomplish these conditions. Finally, the definitive value of the order parameter in the steady state is calculated by performing a temporal average over the points in the range $t \in (9 \cdot 10^3, 10^4)$.

2.5 Parameters and data

To finish, we briefly expose the choice of parameters and data for the dynamical integration. Indeed, the elements that we need to provide are: *i)* birth and death rates, *ii)* mutualistic coefficients, *iii)* initial population, *iv)* periods of activity and *v)* structure of the network.

The first three items are extracted from the parameters used by García-Algarra et al. [9], in their integration of the dynamical equations. Although such parameters are not empirical, their order of magnitude is chosen as to ensure an ecologically realistic value for the growth and carrying capacity of the species. Some tables containing these quantities can be found in Appendix A. In the simulations on the real network and when testing the scaling behaviour, we employ variations over these parameters while keeping its order of magnitude.

Besides, for the period of activity we use two sources of data. In the simulation on the theoretical network we employ a non-empirical yet realistic set of periods, that can be found in Appendix A. Instead, for the real network and the scaling test we use empirical data of periods provided by [8].

Finally, concerning the network structure (apart from the theoretical one, that we have already introduced) we employ the ecological data on mutualistic interactions provided Burkle et al. [8], that will allow us to construct the real network. For the scaling we were inspired in the network compiled by Arroyo et al. [14], available on the ecological network database *Web of Life* [15].

Chapter 3

Results and Discussion

In the previous chapter, a preliminary result suggested that by increasing the strength of the phenological noise we can cause partial extinctions, eventually triggering a transition from a scenario of full survival to one of complete extinction. Motivated by these findings, we now aim to systematically examine the nature of such phase transition.

The discussion is mainly divided in two sections. First, we will attempt to characterise the phase transition by measuring the steady state of the order parameter as a function of the strength of the phenological noise, as well as by performing a test of finite size scaling. Secondly, we study the phase transition on a *real* network (constructed with empirical data) in order to obtain various measures that allow us to explore the implications of our findings to other relevant biological indicators, such as biodiversity or ecosystem's robustness.

3.1 Characterisation of the phase transition

3.1.1 Steady state of the order parameter

Proceeding as explained in *Methods*, we obtain the steady state of the total population n_{st} as a function of σ, as can be seen in Fig. 3.1. The figure clearly suggests the existence of second-order phase transition, since n_{st} changes continuously in the transition. Indeed, we might define n_{st} as the order parameter, because it fulfils properly the classical conditions of being a positive quantity before the critical point and zero beyond [16].

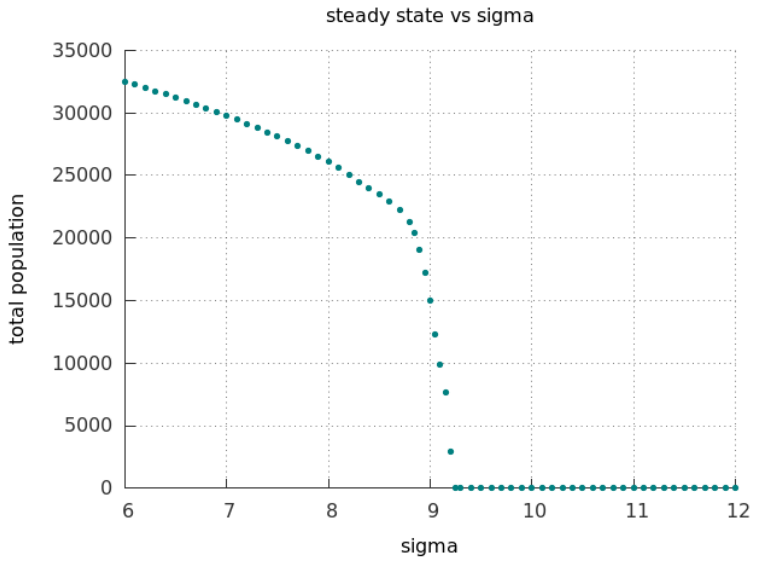

Figure 3.1: n_{st} as a function of σ. The simulation has been realised averaging over 10^4 runs far from criticality and 10^5 runs in the critical region. The integration time is $t_{max} = 10^4$, and the steady state has been calculated averaging over the last 10^3 points of the averaged trajectory.

However, here the notion of order and disorder is not exact. What we actually observe is not a transition from an ordered to a disordered phase, but between an alive, fluctuating state and a dead, absorbing configuration from which the system is unable to scape. This characterises a non-equilibrium phase transition, precisely what is known as an *absorbing phase transition* [13].

Let us be more detailed about this. The equilibrium condition is not fulfilled because, as outlined by [13], the presence of absorbing states breaks the detailed balance condition, placing the process in the land of out-of-equilibrium phenomena. Another way to see it is that, in principle, we can imagine our system to be described by a Langevin equation, in which the phenological mismatch has been introduced as a mutiplicative (and positive) noise affecting the mutualistic coefficients b_{ij}. This should allow for the construction of a time-dependent probabilistic distribution, in the fashion of a Fokker-Planck equation [17] -yet if, as we discussed previously, the treatment of microscopic processes deserves in our case a special care-. Although we will not explore such alternative here, it could be a direction for future investigation.

Non-equilibrium systems are prolific in nature and have been the object of intense study during the last decades [17] [18] [19] [13]. Indeed, it has been shown that some of the essential elements of second-order equilibrium phase transitions, like scaling behaviour or the existence of universality classes, encounter their analogue in non-equilibrium second order phase transitions. Relevantly, among absorbing phase transitions has been found a large universality class called *Directed Percolation*, that gathers models as disparate as epidemic spreading or forest fire, to mention only a few. In the next section we will attempt to perform a finite size scaling on the system, to assert the second-order nature of our transition. Before that, we test the robustness of our result with respect to one of the key modelling aspects: the distribution of initial times.

Effect of the distribution of initial times

In the *Methods* chapter we exposed how one of the important steps of our modelling consists in finding a distribution of initial times for which the overlap is maximum, ensuring that the system reaches the carrying capacity limit. Nonetheless, we could expect that some initial conditions distributions -intuitively, the centred one- will be more resilient to phenological shift than sparser solutions. Therefore it is convenient to test that our results are qualitatively robust regardless of the election of the initial time distribution.

To assert this, in Fig.3.2 we compare three simulations: one with a pseudo-optimal distributions of initial times (produced as explained in section 2.3.), a second one with centred times and a last one averaged over 10^2 different pseudo-optimal initial configurations. Moreover, in the three cases phenological shifts occur only for plants. Observing the figures we can conclude that:

(i) The type of transition is independent of the initial configuration of times, since in the three cases we observe a continuous phase transition. Nonetheless, it does affect the position of the critical point. This should not surprise us, given that this quantity generally depends on the microscopic details of the system [13].

(ii) Centred configuration are more robust (exhibit a larger critical point) than pseudo-optimal ones. This suggests that there must exist a counter-acting factor that favours the sparseness among the periods of activity, probably related to inter-species competition. We will explore further this possibility in the section devoted to the real network.

(iii) Figs. 3.2b and 3.2c are almost identical. In principle, we should expect that the centred direction is the most robust of all. This disagreement with our finding could indicate that the pseudo-optimal distributions are centred in average, yet it is something that should be checked in the future.

(iv) Finally, comparing Fig. 3.2a to Fig. 3.1 we can assert that submitting to phenological noise only a subset of species (plants, in our case) does also produce a second-order phase transition. However, once again the position of the critical point changes and in particular, we encounter the critical region earlier in Fig. 3.1 (that is, if phenological noise affects the whole population).

Consequently, we confirm that our results are robust with respect to the election of the initial configuration of times, ensuring that our findings are not an artefact resulting from a particular choice of initial conditions.

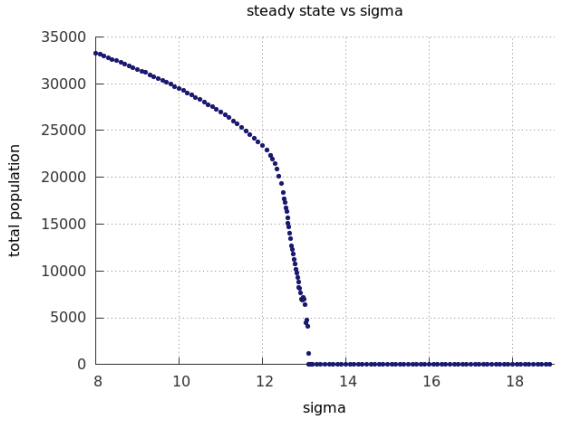

(a) One single pseudo-optimal initial configuration of times.

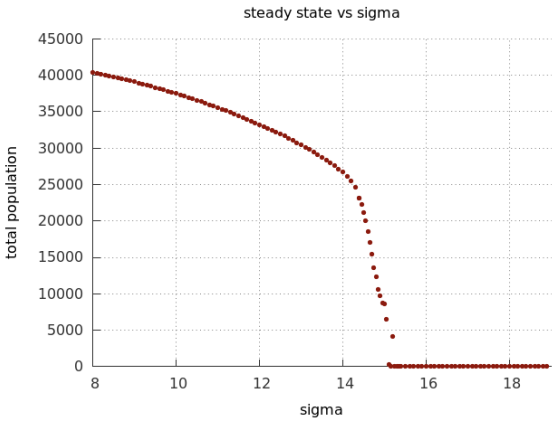

(b) Centred initial configuration of times.

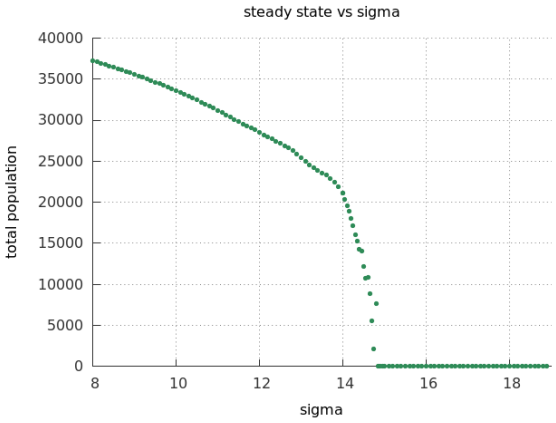

(c) Average over 10^2 pseudo-optimal initial times configurations.

Figure 3.2: Simulations for three different sets of initial times configurations. The steady state has been calculated running 10^5 iterations in the critical region and 10^4 elsewhere. In *c*, we go over 10^2 different pseudo-optimal configurations, meaning that we performed 10^2 repetitions for each set far from the critical region and 10^3 close to it. The rest of parameters, structure of the network and integration time are set as in Fig. 3.1.

3.1.2 Finite size scaling

Our previous analysis suggests that the phase transition that arises due to phenological noise is of second-order type. To assert this result, we now attempt to test whether one of the fundamental features of second-order non-equilibrium phase transitions is fulfilled: specifically, scaling. Owing to the fact that our networks are far from being an infinite-size system, we need to take into account finite-size effects and hence we will perform a *finite-size scaling*.

Methods

To carry out such analysis we need a set of networks that obey the same dynamical rules but differ in their size. In order to warranty such dynamical invariance, we require a null-model network, in which correlations have been erased thus ensuring that its subnetworks will exhibit, in average, the same statistical properties. Since we expect a power-law behaviour, it is convenient that sizes are increasing powers of the same basis. In our case we define the size L as the total number of species $L = N = N_P + N_A$, an employ a two-basis sequence $L = 2, 4, 8, 16, 32, 64$.

To generate the null-network of largest size ($L = 64$) we implement a configuration model without parallel-edges or self-loops. In particular, we use the *bipartite* package from the *NetworkX* library in Python (see [20]). Its configuration-model algorithm takes as an input the number of nodes and its degree distribution and then randomly assigns the edges among the bipartite network so as to reproduce the given degree sequence.

In particular, we employ a semi-empirical degree distribution constructed as follows:

- First, we extract the exact degree sequence from the plant-pollinator network collected by Arroyo et al. [14] (available at [15]) formed by 61 species (36 plants and 25 pollinators) and 81 interactions.
- Then, we add three more species (1 plant and 2 pollinators) and 5 more interactions (in order to keep constant the average degree), thus obtaining the desired network with a total of 64 species and 86 interactions.

The subnetworks of smaller size are then obtained as partial extractions of this null-model. For each size, we select randomly a set of L nodes keeping the appropriate links, and repeat the process until finding a connected subnetwork. This process warrants that there are no isolated nodes, that will surely get extinct. With this we obtain the structures for sizes $L = 32$ (formed by 18 plants and 14 pollinators), $L = 16$ (9 plants and 7 pollinators), $L = 8$ (5 plants and 3 pollinators), $L = 4$ (3 plants and 1 pollinator) and $L = 2$ (1 plant and 1 pollinator).

Finally, we need to assign the dynamical parameters ensuring that all subnetworks work in the full-survival regime and no extinctions occur. To achieve this, we select the parameters randomly from the theoretical values used in the previous chapter (see Appendix *A*). Then, we tune some of them -yet keeping its order of magnitude- until in all networks every specie attains its full-capacity limit. Crucially, these parameters must be preserved across scales, in order to warrant, as much as possible, the same dynamical conditions. In other words, this means that the final assignment of parameters is inherent to each node and link, and saved across subnetworks.

Results

Our hypothesis is that the system exhibits a second-order phase transition and thus some quantities, as explained by [13], behave peculiarly around the critical point σ_c. For instance, in an infinite system the order parameter n_{st} should exhibit a power-law dependence:

$$n_{st} \propto \mid \sigma_c - \sigma \mid^{\beta} \tag{3.1}$$

Being β the so-called order parameter critical exponent. Also, like in second-order equilibrium transitions, the spatial correlation length $\xi_\perp$ diverges with the exponent $\nu_\perp$:

$$\xi_\perp \propto \mid \sigma_c - \sigma \mid^{-\nu_\perp} \tag{3.2}$$

In addition, in a non-equilibrium phase transition time is also degree of freedom. Thus we need to consider the divergence of a second correlation length $\nu_\parallel$, now of temporal nature:

$$\xi_\parallel \propto \mid \sigma_c - \sigma \mid^{-\nu_\parallel} \tag{3.3}$$

Which would allow as well for a dynamic scaling analysis [13]. Anyway, we are now interested in the scaling of the steady state of the order parameter, that is, in testing the validity of Eq. 3.1. For this, we need to bear in mind that the mentioned relations are thought for an infinite system.

In a finite size network like ours, the spatial correlation length can not actually diverge but is restricted by the extension of the system. This means that when we are sufficiently near to the critical point, L an ξ may become comparable and all our measures will be conditioned by the particular size of the system. Hopefully, not everything is lost and we can appeal to the finite-size scaling hypothesis.

It consists in assuming that all quantities depend actually in the variable: $\mid \sigma_c - \sigma \mid L^{1/\nu_\perp}$. Therefore the steady state can be expressed as a function of both the distance to the critical point and the size as:

$$n_{st}(\sigma, L) \propto L^{-\beta/\nu_\perp} f((\sigma - \sigma_c)L^{1/\nu_\perp}) \tag{3.4}$$

And so when we are on the critical point we obtain:

$$n_{st}(\sigma_c, L) \propto L^{-\beta/\nu_\perp} \tag{3.5}$$

Which is once again a power-law dependence. In a similar fashion to the analysis of the critical behaviour of the pair-contact process by Jensen [21], we plot the density steady state of the system as a function of L, for different values of our control parameter σ. In a log-log plot, this should lead us to a straight line when we are exactly on the critical point, as indicates Eq. 3.5. In the region where $\sigma > \sigma_c$, we expect that the points will decay faster than a power-law, since all sizes have entered the absorbing state. For $\sigma < \sigma_c$, the steady state should not depend on the size of the system if $L \gg \xi_\perp$, thus leading to a flat behaviour. Crucially, systems with $L \sim \xi_\perp$ will enter the absorbing state even for $\sigma < \sigma_c$. Given that our systems sizes are small, this is an essential source of error to take into account.

In order to be able to compare the measures of n_{st} across different scales, we define the intensive quantity ρ_{st}. This density is calculated by dividing the steady population as explained in *Methods*, by the total carrying capacity of the system at that size, that is: $\rho_{st} = n_{st}/n_{car}$. Intuitively, ρ_{st} can be understood as a measure of the concentration, that is, the total number of occupied sites (alive individuals) over the total number of available sites (carrying capacity).

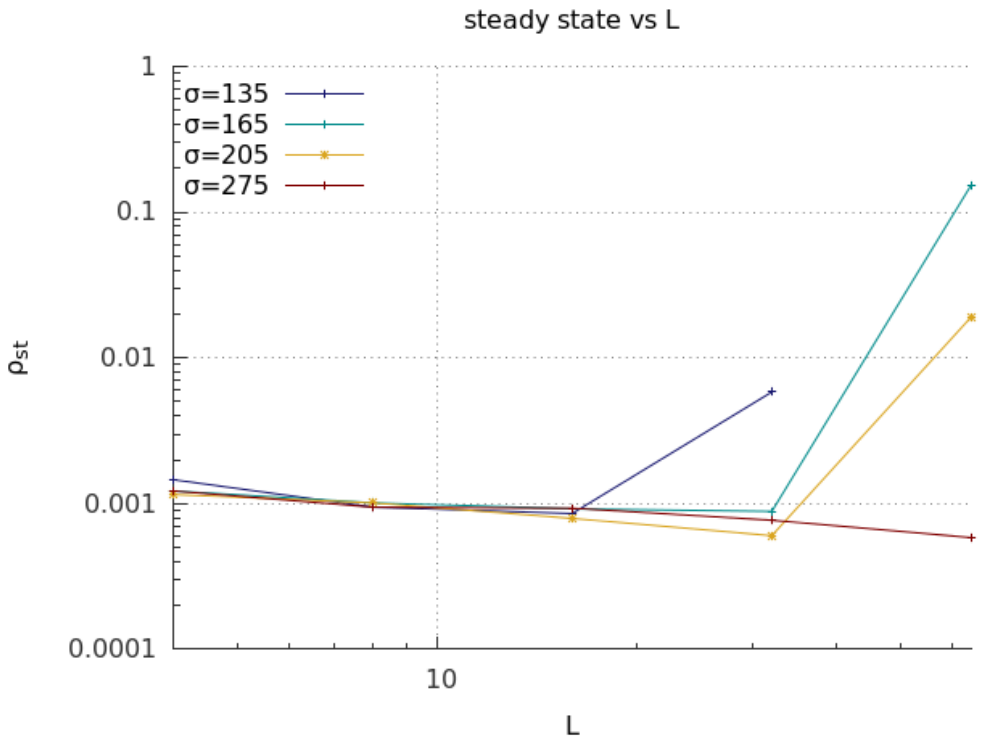

Figure 3.3: Density of the steady state ρ_{st} as a function of the network size for different values of σ. The point for $L = 2$ was finally not included since it was not significant. The number of iterations performed was 10^5 for $L = 4, 8$, 10^4 for $L = 16, 32$, and finally $5 \cdot 10^2$ for $L = 64$. Points are united among them by lines in order to facilite the understanding of the tendency.

In Fig. 3.3 we show the log-log plot of ρ_{st} versus L. From this result, our first conclusion is that the scaling behaviour can not be asserted. According to the theory of finite size scaling the critical

point has approximately the value $\sigma \simeq 275.0$ days, which is the point at which the absorbing state has been reached in all sizes and we get a straight line. However, this value differs strongly among smaller systems, that can be observed to reach the absorbing state much earlier.

This divergence could be due to a variety of reasons. First and most relevantly, the system sizes were probably too small for our purpose, leading to rapid absorptions and not fulfilling that $L \gg \xi_{\perp}$. Secondly and related to this, measuring the steady state accurately was incredibly difficult. The population dynamics exhibits critical slowing down near the critical point, meaning that different species (coming from different carrying capacities) reach their steady state at different points, as seen in Fig. 3.4a. Adding to this the fact that the system gets absorbed rather quickly, we often encountered a situation where some species had yet not reached its steady state, while others have already been absorbed (see Fig. 3.4b). In this scenario, discerning between a genuine absorbing steady state and an small but still active state that has been absorbed due to fluctuations becomes impossible. In the whole, all this makes the analysis considerably intricate and poorly systematic.

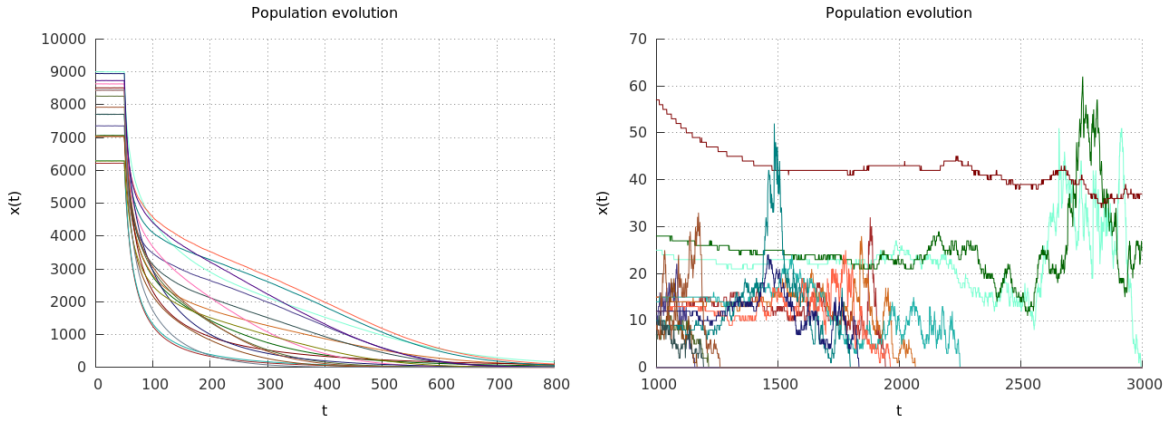

(a) Averaged trajectories for plants with $L = 32$ and $\sigma = 155$.

(b) Averaged trajectories for plants with $L = 32$ and $\sigma = 275$.

Figure 3.4: In *a*, time evolution of the averaged trajectories for plant species, showing that those coming from larger carrying capacities take more time to reach the steady state. Near the critical point, this effect is enhanced due to critical slowing down. In *b* , trajectories for plant species showing absorptions at different times.

Nevertheless, in perspective the results are not so discouraging. In this section we showed that the system exhibits a phase transition when subject to an increasing phenological noise. The phase transition seems to be of second-order type, and we have proposed a way to analyse its critical behaviour. Although our results regarding scaling are not conclusive, they may serve to learn how to enhance the quality of our measures, opening the door to further research. Beyond this finite-size scaling there is left to explore a whole world of critical exponents and universality classes. Indeed, fully characterising this phase transition might be an interesting question not only regarding its ecological implications, but also from the physical point of view of non-equillibrium phase transitions, which are nowadays object of a lively interest.

3.2 Phase transition on a real network

In this section we analyse the phase transition and its ecological consequences on a network constructed using the empirical data collected by Burkle et. al [8], available at [22].

This dataset comprehends information about a community of plant-pollinators in a temperate forest in Illinois, USA. As we mentioned in the introduction, Burkle et al. recorded the phenology and structure of interactions among forbs and bees in 2009-2010, and then compared it with a historical dataset gathered, on the same region, by Charles Robertson in the late 1800s. Their published data contains the following information: network structure of interactions in 2009-2010 and edge's weight (number of visits observed per link), dates of start and end of activity in 2009-2010 and start and end dates in Robertson times.

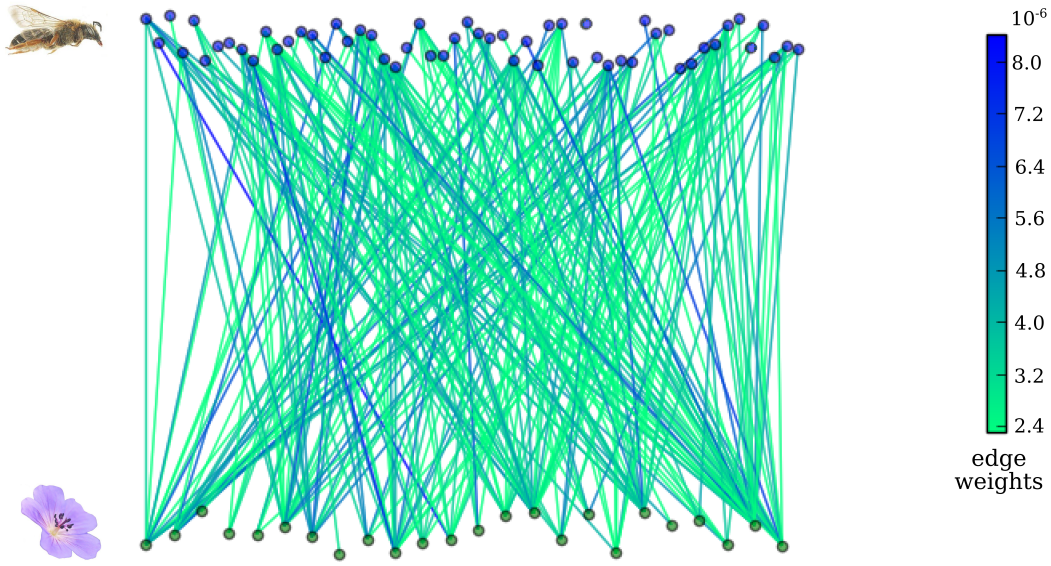

Figure 3.5: Graphical representation of the real network. Above, bee species labelled by a picture of the *Halicatus Rubicundus*, one of the involved pollinators. Below, plants nodes and a picture of the *Geranium maculatum*, one of the forbs' species forming part of the network. The color range used to represent the weight of the link b_{ij} is in logarithmic scale, in particular we mapped $log(10^7 \cdot b_{ij})$ to the colors.

To construct the network we used the set of interactions as registered in 2009-2010, formed by 24 species of plants and 54 species of bees (see Fig. 3.4). Unfortunately, the corresponding phenological information from 2009-2010 is insufficient for our purpose, since some of the end dates in the available data are missing. Given that we need the period of activity, we employed instead the phenologies for the same species as recorded by Robertson in 1800s. This is not the optimal procedure, since the perfect coherence with the empirical network is lost. All in all, the impact on our results should not be severe. Considering that Burkle et al. showed that periods were longer in the 1800's, the expected effect is only a moderate enhancement of the resilience to phenological shifts.

About the dynamical parameters, we set the growth rates and the initial populations by randomly selecting among the dynamical values used for the theoretical integration (see tables in Appendix A), and then tuning some of them -yet keeping its order of magnitude- so as to guarantee the dynamical regime of full capacity. Mutualistic coefficients b_{ij} were assigned by converting to a realistic order of magnitude (10^{-5}-10^{-6}) the number of observed pollinator's visits per interaction. This does not mean that the weights of the links are empirical, but at least they are inspired on the experimental data.

In the end, this provides us with a network constructed from a real set of interactions and periods. Our aim is to simulate its dynamics under the effect of phenological noise and, more importantly, to interpret biologically our results in order to understand its ecological significance and relate it with the current discussion on mutualistic networks.

3.2.1 Discussion on the transition

We start by obtaining the steady state of the total population n_{st} as a function of the strength of the phenological noise σ, following the procedure described in *Methods*. This leads us to a non-equilibrium phase transition to an absorbing state, as we can observe in Fig. 3.6.

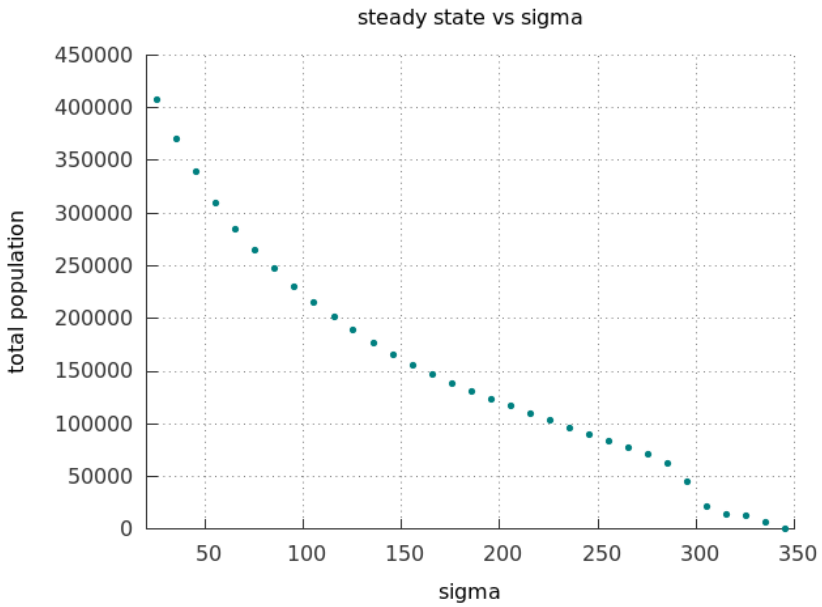

Figure 3.6: Steady state of the total population as a function of the noise amplitude σ. Simulations performed on the real network shown in Fig.3.3. I carried out 10^3 iteration per point and the final integration time is $t = 10^4$ years. The configuration of initial times is a pseudo-optimal solution of the optimizing period.

The figure suggests once again that the phase transition is of second-order type. Despite the fact that we could not confirm this result convincingly in the previous section, we still can explore what physical and biological explanations may support the existence of this type of transition. In particular, for a non-spatially extended like ours, there are mainly two elements conditioning the way in which a network collapses: *i)* the dynamics of interaction and *ii)* the topology of links.

From **(i)**, the **dynamical point of view**, the existence of a continuous critical transition seems to be a plausible possibility. A first reason is that our interactive scheme presents some resemblance with the Pair-Contact process [23]. In such system, pairs of particles may encounter each other so as to either annihilate one another, either reproduce by filling a vacant nearest neighbour. However, there are also some significant differences that could completely invalidate our analogy, in short: the bipartite nature of mutualistic interaction, the existence of intraespecific competition and the non-random structure of interactions.

The second argument is related with universal classes in non-equilibrium systems. As we mentioned in the previous section, absorbing phase transitions contain a huge universality class called *Directed percolation*. The variety of disparate models belonging to this same universality class was so outstanding, that eventually it was proposed the so-called *DP-conjecture*. It states that a given model will generally belong to the DP- class when it fulfils that:

1. It exhibits a second-order phase transition between a fluctuating active phase and a unique absorbing state
2. Its order parameter is non-negative and one-component
3. Dynamic rules are short-ranged
4. The system shows no special attributes such as unconventional symmetries or conservation laws

In our model, the second item is satisfied. The third point is not fullfilled since mutualistic interactions involve many partners, thus resulting in non-local dynamics with long-range effects. Also,

the fourth point might be violated by the embedding of our system in a network of interactions. Still, other processes also framed in networks such as epidemic spreading proved to belong anyway to the DP-class, revealing that this condition is not strictly necessary. About the first item, the transition to an absorbing state was fulfilled, but we could not assert its scaling behaviour. On the whole, what we aim to suggest is that our system possesses many common features with other models exhibiting second order-transitions. Even if, obviously, this does not allow us to state that the transition is actually of second order (even less to say it belongs to the DP-class), the encountered similarities provide, not blindly, a certain plausibility of obtaining such solution.

Factor **(ii)**, the **topology of links**, offers counteracting arguments. On the one hand, the distributions of links is known to hold a scaling behaviour, in particular due to a truncated power-law [24]. Returning again to the percolation analogue but now in scale-free networks, we can recall that it results as well in a continuous phase transition. On the other hand, the singular correlations underlying mutualistic network's structure may encode essential information such as the phylogenetic signal, that cause structured cascade of extinctions and besides highly non-linear responses. This might eventually lead to abrupt evolutions indicating the existence of tipping-points and a first order transition.

In the end, this discussion is not aimed at more than providing a rather speculative overview of the type of arguments that might support one type of transition or the other. Eventually, the final answer can only be attested by further evidence on the scaling behaviour.

3.2.2 Reencounter of relevant ecological traits

Our aim is now to adopt a biologically focused perspective, carrying out a broader analysis that allows to recognise typical patterns and features of plant-pollinators networks. With this idea in mind, we plot, first, the number of alive species in the steady state versus the strength of the phenological noise σ, found in Fig. 3.7. Then, the nestedness of the steady network at a certain value of σ, as shows Fig. 3.8. And finally in Fig. 3.9, the degree of a node versus the value of sigma at which it gets extinct for the first time. The three measures where performed on the data obtained by the simulation of Fig. 3.6. From the comparison among the different results for the real network, we may drive the following bare observations (which we will later discuss and justify):

(i) The evolution of the steady state shows a sort of plateau before its critical transition. Such region coincides with a period of absence of extinctions and, crucially, a significant recovery of the nestedness of the network (with respect to immediately precedent configurations).

(ii) The extinction of large-degree nodes seem to obey a positive correlation with σ. On the contrary, low-degree nodes get extinct quite uniformly through the transition

(iii) The critical transition occurs at the same σ_c at which a massive extinction of nodes occurs (involving large-degree species), coinciding as well with a sharp drop of the nestedness

The first conclusion that arises from finding *(i)* is the fact that local extinctions do not necessarily need to drive the network to less resilient configurations, but might occasionally collapse to more nested structures. This possibility was already conceived by García-Algarra et al. [9], as we reviewed in *Methods*. Such result outlines how nestedness accounts for a genuinely global quality of the system, that might be recovered even after partial extirpations of the network, thus suggesting the existence of structural self-similarity at various scales.

In addition, such special organization of links reveals once again to provide an enhanced resilience to the system. Indeed, specialist species are capable of resisting intense perturbations thanks to their interactions with highly stable generalist species, as suggested in [1], as here we observed in *(ii)*. In the end, the disappearance of the residual core of generalists and its attached species results in the decisive transition to the global absorbing state *(iii)*. This suits the idea from Jordano et al. [24] that thanks to the truncated power-law that follow the distribution of links, plant-pollinator networks manifest a featured robustness similarly to scale-free networks. Actually, as outlined by [24], even enhanced by a natural mechanism that restricts the formation of hubs, which would dramatically increase the vulnerability of the network to targeted attacks.

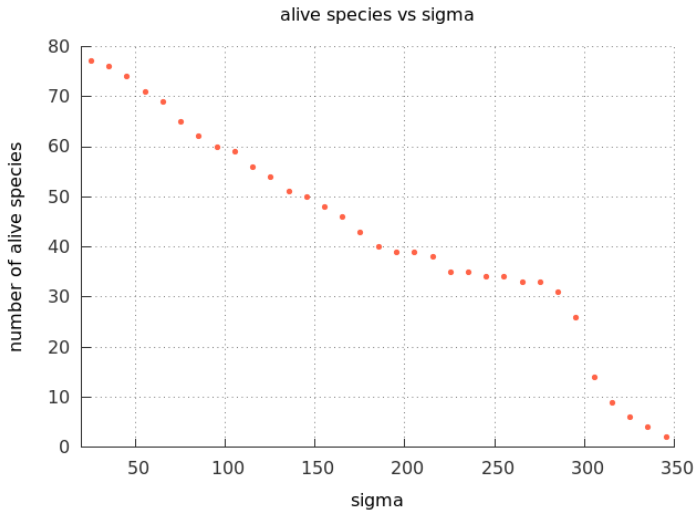

Figure 3.7: Number of alive species in the steady state as a function of the phenological noise applied to the network.

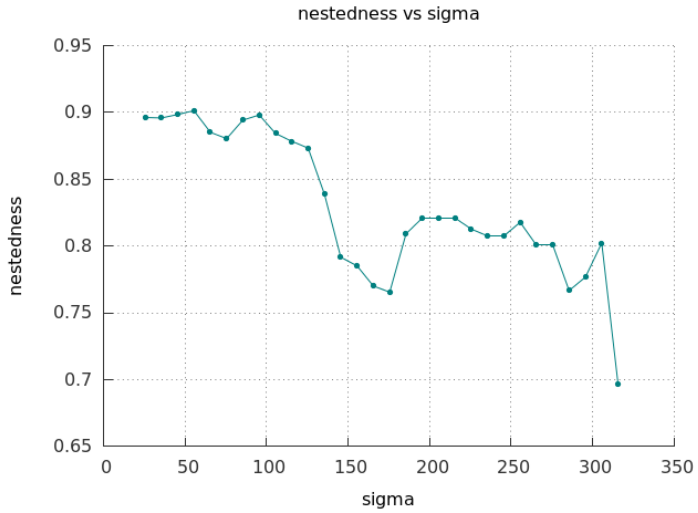

Figure 3.8: Nestedness of the steady network as a function of the strength of the phenological noise. To calculate the nestedness of the networks we employed the program *BINMATNEST* [25] .

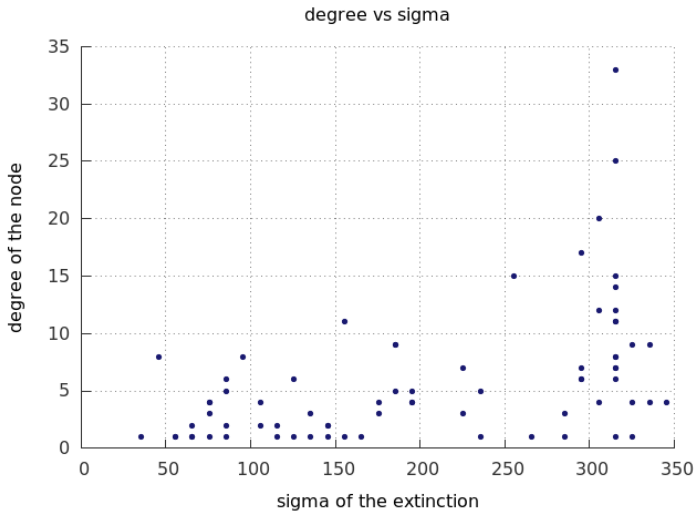

Figure 3.9: Degree of a node (initial) versus sigma at which it gets extinct for the first time.

Crucially, such reproduction of well-known ecological properties provides an indirect assurance of the solid grounds underlying our procedure. Knowing this, our next section will be devoted to making some further considerations on the information provided by the transition, now regarding quantitative predictions.

3.2.3 Quantitative significance of the results

Given that we have employed a combination of experimental and realistic (yet theoretical) parameters, we might expect our findings to be empirically faithful, at least in its order of magnitude. The most relevant quantity related to the observed phase transition is the critical point, σ_c. From Fig. 3.6 we obtain an estimated value of $\sigma_c \approx 300$ days. Strikingly, this means that in order to trigger a complete extinction of the network under our study, we would require a phenological variability with an amplitude longer than three quarter parts of a year. Namely, the disappearance of seasonality.

In fact, this quantity can by no means be considered universal, since the critical point is in general sensitive to the concrete arrangements of a system. In spite of that, this outcome poses the question of what dependence exists between the parameter region used for our simulation and the quantitative behaviour of our system. To address this question extensive explorations of the parameter space would be needed, which unfortunately we did not have time to perform.

3.2.4 Beyond mutualism: interspecific competitions

Finally, we close this section together with the chapter by presenting a collateral observation on the data, connected with an earlier exploration on the theoretical network that concerned the distribution of initial times.

Specifically, we previously showed that non-random patterns in the configuration of the birth and flowering dates lead, on otherwise identical networks, to diverging values of the critical point. Centred distributions offer an enhanced robustness, whereas single random configurations are more vulnerable to phenological noise.

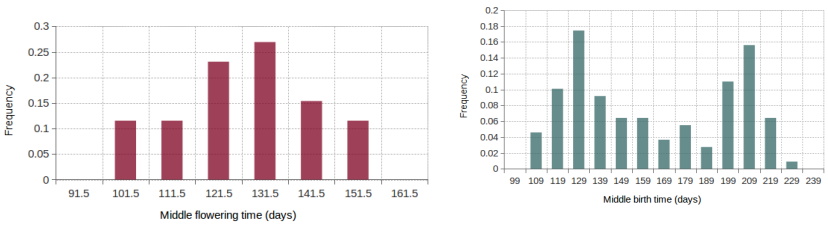

(a) Plants.

(b) Bees.

Figure 3.10: Histograms of the distributions of the middle time of activity for plants and its pollinators, extracted from the historic data set by [8].

We would expect that if no other interactions apart from mutualism are relevant, then initial time configurations should be centred, because such arrangement is optimal with regard to resilience to phenological shifts. On the contrary, the empirical distributions extracted from the network by Burkle et al.[8] do certainly not posses such centred pattern, as reveal Fig 3.10a and Fig. 3.10b.

This suggests that interactions of a distinctive nature might be contributing to the peculiar organization of species' phenology. In other words, there must exist a counter-interaction harmful for species activity, whose effect is palliated by the sparness of phenologies. Thus the observed distribution might result from a balance between the decrease in resilience and a mitigation of this damaging factor. At first sight, the most probable candidate for such role is a competitive interaction.

In fact, in the beginning we reviewed how interspecific competitions are an unavoidable component to understand the assemblage of nested structures [3]. In light of our results, they might also be related with why species tend to act dispersedly in time rather than fully synchronised.

Chapter 4

Conclusions and Perspectives

The results of this Master Thesis assert that systems undergoing mutualistic alterations due to the presence of phenological noise eventually suffer a transition into global extinction. Moreover, it was suggested that such transition of of second-order type thanks to the characterisation of the steady state of the order parameter as a function of the noise strength. Yet, our test of finite size scaling was not concluding, and therefore we could not entirely confirm whether this was certainly the nature of the transition.

Additionally, we carried out the simulations and analysis on an empirically constructed network, that lead as well to a continuous phase transition. Besides, we extended our study in order to depict the evolution of some characteristic network's features, such as the nestedness and the degree of the nodes. This procedure permitted us to recover essential ecological traits, thus building a first bridge between the dynamical description provided by our model and some well-established properties of mutualistic networks.

During the discussion, many directions of future exploration have already been suggested. The most pressing and probably prolific one is the full characterisation of the phase transition. Indeed, proving scaling would have strong implications on our understanding of the critical behaviour of the system, opening the door to the measurement of critical exponents and even a classification within universality classes. Without going that far, other perspectives of investigation may include studying the dependence to the parameters or testing more sophisticated models of interaction, for instance, one accounting for inter-specific competition.

In more general terms, an alternative path for developing the methodology here presented is to detach the notion of noise from the particular framework of phenological shifts. Instead, we could study the robustness of the network to a generalised stochastic degradation of mutualistic interactions. Technically, both approaches are exactly equivalent. Nevertheless, this change of interpretation might bring to the discussion new ideas and perspectives.

Appendix A

Tables of parameters

	Plant 1	Plant 2	Plant 3	Plant 4
Pol 1	(14,1)	(12,12)	(2,12)	(10,16)
Pol 2	(13,12)	(6,4)	(5,11)	(1,0)
Pol 3	(10,12)	(1,10)	(1,0)	(0,0)
Pol 4	(10,6)	(10,10)	(0,0)	(0,0)
Pol 5	(20,10)	(0,0)	(0,0)	(0, 0)

Table A.1: Matrix of the benefit due to mutalistic interactions $b_{kl}(10^{-6})$. As can be observed, the matrix is not symmetric. The left term inside the brackets, b_{ij}, represents the benefit reported to pollinator i due to its interaction with plant j. The second term, b_{ji}, represents the benefit to plant j due to its interaction with pollinator i.

	r	α (10^{-6})	c (10^{-4})
Pol 1	-0.016	10	1
Pol 2	-0.038	10	1
Pol 3	-0.015	8	1
Pol 4	-0.014	10	1
Pol 5	-0.018	30	1
Plant 1	-0.001	7	1
Plant 2	-0.03	12	1
Plant 3	-0.04	12	1
Plant 4	-0.0005	10	1

Table A.2: Parameters of growth r, intraespecies competition α and the coefficient for the frictional dependence with mutualism c.

.

	Pol 1	Pol 2	Pol 3	Pol 4	Pol 5
N_i	500	300	500	200	150
	Plant 1	Plant 2	Plant 3	Plant 4	
N_j	700	600	500	200	

Table A.3: Initial values of the populations in the case of complete extinction.

	Pol 1	Pol 2	Pol 3	Pol 4	Pol 5
N_i	700	600	1000	700	500
	Plant 1	Plant 2	Plant 3	Plant 4	
N_j	1500	2000	1200	1500	

Table A.4: Initial values of the populations in the case of full capacity.

Bibliography

[1] J. Bascompte, P. Jordano, C. J. Melián, and J. M. Olesen, "The nested assembly of plant–animal mutualistic networks," *Proceedings of the National Academy of Sciences*, vol. 100, no. 16, pp. 9383–9387, 2003.

[2] J. Bascompte, P. Jordano, and J. M. Olesen, "Asymmetric coevolutionary networks facilitate biodiversity maintenance," *Science*, vol. 312, no. 5772, pp. 431–433, 2006.

[3] U. Bastolla, M. A. Fortuna, A. Pascual-García, A. Ferrera, B. Luque, and J. Bascompte, "The architecture of mutualistic networks minimizes competition and increases biodiversity," *Nature*, vol. 458, no. 7241, pp. 1018–1020, 2009.

[4] E. L. Rezende, J. E. Lavabre, P. R. Guimarães, P. Jordano, and J. Bascompte, "Non-random coextinctions in phylogenetically structured mutualistic networks," *Nature*, vol. 448, no. 7156, pp. 925–928, 2007.

[5] E. Thébault and C. Fontaine, "Stability of ecological communities and the architecture of mutualistic and trophic networks," *Science*, vol. 329, no. 5993, pp. 853–856, 2010.

[6] S. J. Hegland, A. Nielsen, A. Lázaro, A.-L. Bjerknes, and Ø. Totland, "How does climate warming affect plant-pollinator interactions?," *Ecology Letters*, vol. 12, no. 2, pp. 184–195, 2009.

[7] J. Memmott, P. G. Craze, N. M. Waser, and M. V. Price, "Global warming and the disruption of plant–pollinator interactions," *Ecology Letters*, vol. 10, no. 8, pp. 710–717, 2007.

[8] L. A. Burkle, J. C. Marlin, and T. M. Knight, "Plant-pollinator interactions over 120 years: loss of species, co-occurrence, and function," *Science*, vol. 339, no. 6127, pp. 1611–1615, 2013.

[9] J. García-Algarra, J. Galeano, J. M. Pastor, J. M. Iriondo, and J. J. Ramasco, "Rethinking the logistic approach for population dynamics of mutualistic interactions," *Journal of Theoretical Biology*, vol. 363, pp. 332–343, 2014.

[10] D. T. Gillespie, "Exact stochastic simulation of coupled chemical reactions," *The Journal of Physical Chemistry*, vol. 81, no. 25, pp. 2340–2361, 1977.

[11] R. Toral and P. Colet, *Stochastic Numerical Methods: An Introduction for Students and Scientists*. Weinheim, Germany: Wiley-VCH, 2014.

[12] D. SciPy, *Differential Evolution Package*. Available at `http://docs.scipy.org/doc/scipy/reference/generated/scipy.optimize.differential_evolution.html`.

[13] M. Henkel, H. Hinrichsen, S. Lübeck, and M. Pleimling, *Non-equilibrium phase transitions*, vol. 1. Springer, 2008.

[14] M. T. K. Arroyo, R. Primack, and J. Armesto, "Community studies in pollination ecology in the high temperate andes of central chile. i. pollination mechanisms and altitudinal variation," *American Journal of Botany*, pp. 82–97, 1982.

[15] B. Lab, *Web of Life, ecological networks database*. Available at `http://www.web-of-life.es/`.

[16] J. M. Yeomans, *Statistical mechanics of phase transitions*. Clarendon Press, 1992.

[17] R. Balescu, "Equilibrium and nonequilibrium statistical mechanics," *John Wiley and Sons, New York*, 1975.

[18] H. Hinrichsen, "Non-equilibrium critical phenomena and phase transitions into absorbing states," *Advances in Physics*, vol. 49, no. 7, pp. 815–958, 2000.

[19] J. Marro and R. Dickman, *Nonequilibrium phase transitions in lattice models*. Cambridge University Press, 2005.

[20] D. NetworkX, *Bipartite Package*. Available at `https://networkx.github.io/documentation/development/reference/algorithms.bipartite.html/`.

[21] I. Jensen and R. Dickman, "Nonequilibrium phase transitions in systems with infinitely many absorbing states," *Physical Review E*, vol. 48, no. 3, p. 1710, 1993.

[22] L. A. Burkle, J. C. Marlin, and T. M. Knight, *Data from: Plant-pollinator interactions over 120 years: loss of species, co-occurrence, and function*. Available at Dryad Digital Repository: `http://dx.doi.org/10.5061/dryad.rp321`.

[23] I. Jensen, "Critical behavior of the pair contact process," *Physical Review Letters*, vol. 70, no. 10, p. 1465, 1993.

[24] P. Jordano, J. Bascompte, and J. M. Olesen, "Invariant properties in coevolutionary networks of plant–animal interactions," *Ecology Letters*, vol. 6, no. 1, pp. 69–81, 2003.

[25] M. Á. Rodríguez-Gironés and L. Santamaría, "How foraging behaviour and resource partitioning can drive the evolution of flowers and the structure of pollination networks," *Scientific Research Publishing*, 2010.